infrastructures

Article

Preliminary Evaluation of Geopolymer Mix Design Applying the Design of Experiments Method

Sergio Copetti Callai *, Piergiorgio Tataranni and Cesare Sangiorgi

Department of Civil, Chemical, Environmental and Materials Engineering, University of Bologna, 40136 Bologna, Italy; piergiorg.tataranni2@unibo.it (P.T.); cesare.sangiorgi4@unibo.it (C.S.)
* Correspondence: sergio.copetticalla2@unibo.it

Abstract: The use of waste materials in road construction is becoming widely spread due to economic and environmental needs. Construction and demolition waste materials and mining residues have been studied for a long time. However, the use of fine materials, mainly from mine tailing and mining residue, is still complex, as they can be used as inert materials into the mix or can become a reactive agent in geopolymer mixes. In the present paper, an experimental application of basalt powder is proposed in the geopolymerisation reaction to produce artificial aggregates. In order to understand the input and output variables' interactions used in the mix design, a statistical method called Design of Experiments was applied. With this design approach, it was possible to optimize the mix design of the experimental geopolymer mortars. The study evaluated several mixes with respect to their workability, compressive strength, and success rate of aggregates production. Finally, a model for predicting compressive strength is proposed and evaluated.

Keywords: design of experiments; geopolymer; artificial aggregates; mixture design; waste powder recycling

Citation: Copetti Callai, S.; Tataranni, P.; Sangiorgi, C. Preliminary Evaluation of Geopolymer Mix Design Applying the Design of Experiments Method. *Infrastructures* **2021**, *6*, 35. https://doi.org/10.3390/infrastructures6030035

Academic Editor: Carlos Morón Fernández

Received: 4 February 2021
Accepted: 25 February 2021
Published: 4 March 2021

1. Introduction

The road construction industry is targeting greener solutions, and aggregate recycling has now become a necessary approach for many authorities and practitioners; for instance, a number of research projects and pilot trials are aiming to achieve consistent pavement performance when recycling up to 100% of reclaimed asphalt concrete. A broad set of other projects worldwide are dealing with the recycling of construction and demolition waste materials [1–3]. Nevertheless, aggregate quarries must still keep up with the global demand for virgin aggregates, especially required to construct the road surface layers with specific features (porous asphalt, stone mastic asphalt, microsurfacings, etc.) [4]. In this context, regarding the plant production processes for aggregates, the milling and crushing stages are usually followed by screening and washing prior to final stockpiling. Large amounts of mineral wastes are often produced, and therefore, it is important to research alternative solutions to reduce their impact on the environment. These waste materials, mostly mineral powder from plant processes, are becoming an environmental issue that requires landfilling limitations and strict legislation on their disposal [5].

Most of these fines cannot be directly used in cement concrete, cement bound layers, or bituminous layers, as they do not meet the requirements of the technical specifications, which are generally based on virgin materials' properties. Therefore, they need to be characterized according to the EN 13043, which specifies the properties of the aggregate' for road applications [6]. In some cases, their direct use might hinder the strength and durability of the construction materials. In other cases, their recovery and recycling can be difficult and not economically feasible. However, some interesting and promising results have been obtained [7–9].

In the stream of the mentioned recycling approaches and, in order to overcome the above limitations and provide an alternative use to the scrap fine minerals, emerging solutions make use of the geopolymerisation techniques. These foresee the recycling of waste powders, known as precursors, in the alkali activation process provided by selected activators [5,10–12].

Examples of this approach exist and aim to instill additional value to the waste powders, using them as precursors to produce engineered artificial aggregates (either dense or expanded). These aggregates provide specific functionalities to the constructed layers while replacing the virgin natural materials. Artificial aggregates from the authors have shown interesting results when designed to increase friction and reduce noise in urban paving solutions [13–15]. Some studies were conducted to assess the use of artificial geopolymeric aggregates with interesting results regarding the physical characteristics [16,17].

The world of geopolymers is expanding, and different applications are today possible in various engineering fields, which find them suitable for their properties [11–13]. In parallel, a number of studies have assessed the environmental footprint of the geopolymers in comparison with traditional materials, e.g., cement concrete. The use of life cycle sssessment (LCA) methodologies is helping to identify the actual benefits of this recycling approach towards a fully circular economy, with the obtained materials being re-recyclable.

The present research aims to characterize a geopolymer mix made of basalt powder to create artificial aggregates that have been designed into a specific shape that could tackle both noise and skid resistance issues in urban road surfaces. For this purpose, a statistical tool called Design of Experiments (DoE) was adopted to select the most suitable mix design, based on the material workability and strength and the success rate in the production of the artificial aggregates.

2. Materials

Geopolymers are synthesized by chemical reactions between silicates and aluminosilicate precursors under strongly alkaline conditions. These reactions lead to the creation of Si−O−Al−O polymeric bonds. Geopolymerisation is an alkali-activation process that changes vitreous structures (either partially or totally amorphous and/or in a metastable state) into a compact cementitious compound [18,19]. The inner structure of geopolymers and their properties depend mostly on the nature and proportions of the material's origin, the curing time and temperature, and the alkaline activators [19]. In fact, they are also called activators because they provide the highly alkaline medium necessary to dissolve silica and alumina. These alkaline activators are also responsible for stimulating the precursor materials' hydraulic properties in the process [18].

Geopolymer nanostructure has been the focus of many types of research, despite not being fully understood yet due to its extreme complexity [20]. The geopolymer material is composed of a mix of activators and precursors. Activators are alkaline liquids responsible for dissolving the precursors' structure and form a brand new structure. Precursors are usually mineral powders that, when dissolved into an alkaline solution, react and, depending on their origin, will provide different characteristics in strength, finishing quality, and others.

Typically, the geopolymer design is made on a trial-and-error basis, mixing different precursors and activators' ratios. This method is used because the chemical reaction is very complex, and the materials used as precursors might not have a specific characterization. However, it is possible to use the theory from [21] to have a specific mix that, using the chemical components from the activators and precursors, allows the geopolymers' production.

2.1. Experimental Materials

As described above, the geopolymer mortar is an alkali-activated mix of activators and precursors. The activators are usually liquid and mixed in an alkaline solution with precursors, which are raw materials (powders) rich in alumino-silicate oxides and with selected reactivity. These components' reactions generate the geopolymer paste that, under specific curing conditions, becomes strong and durable enough to behave as a construction material for civil engineering purposes

2.1.1. Activators

The adopted activators are a mixture of liquid sodium silicate (SS) and sodium hydroxide (SH). Sodium silicate (SS) (Na_2SiO_3), also commonly known as water glass, is an aqueous solution of sodium oxide (Na_2O) and silicon dioxide (SiO_2) mixed according to specific proportions. A solution can be obtained with different properties by changing the ratio between SiO_2 and Na_2O; the solution is suitable for several applications, from the construction to the food field. The SS employed in experimentation is a commercial product, with a SiO_2/Na_2O ratio of 1.99 and a viscosity of 150–250 MPa·s at 20 °C.

Sodium hydroxide (SH) (NaOH) is a very basic NaOH solution, which allows the dissolution of the aluminosilicates. It increases the pH, and it compensates for the electric charge of the aluminates in the mixture. It is an inorganic compound that is a highly caustic base and highly soluble in water. A 10 M SH was used in the present work.

2.1.2. Precursors

Different precursors have been used in various research studies, among them fly ash [22], metakaolin [5], and blast furnace slag [23]. The type of precursor has a direct impact on many mechanical and chemical properties of geopolymers. Inert waste dust could act as a filler/aggregate in the geopolymer structure. On the other hand, a reactive amorphous waste could act as a precursor in the geopolymer matrix. Therefore, studying the precursors' mineralogy is vital to understand its constituent species and possible reactivity [5]. The materials used in this paper were metakaolin and basalt powder.

2.1.3. Metakaolin Powder

Calcined kaolinitic clays, otherwise known as metakaolin (MK), were one of the first precursors used in geopolymer research. MK's initial application was mainly in paper and plastic industries, where it was used as filler. The composition of metakaolin is mainly made of SiO_2 and Al_2O_3 with a small percentage of metal oxides [21].

When used in cement concrete applications, MK increases the compressive and flexural strength of concrete, reduces its permeability, increases its resistance to chemical attack, enhances the workability, and increases the durability of the concrete [24]. Geopolymers can benefit from the MK qualities, especially as it has a high Al_2O_3 content, being very reactive to the activators [25–27]. In the present work, it was used a commercial metakaolin with a size passing 0.063 mm sieve.

2.1.4. Basalt Powder

The basalt powder is a residual from the extractions and production processes in trachyte quarries. As volcanic rocks, basalt deposits are present in almost every country. This lithotype is widely used, depending on each deposit's intrinsic characteristics, in the construction field for its mineralogical, chemical, and physical properties. The extensive use of this material for bituminous mixtures and concretes leads to the production of large quantities of sands and powders during the crushing of aggregates [5]. The basalt powder's chemical composition is presented in Table 1, based on the Reference Intensity Ratio (RIR) method for a semi-quantitative estimate with 10–20% error.

Table 1. Chemical composition of the basalt powder (Reference Intensity Ratio (RIR) method).

Name	Composition	Percentage
Leucite	$(K(AlSi_2O_6))$	44
Augite	$((Ca,Mg,Fe)_2Si_2O_6)$	17
Anorthite	$(Ca(Al_2Si_2O_8))$	12
Orthoclase	$(K(AlSi_3O_8))$	5
Muscovite	$(KAl_2(Si_3Al)O_{10}(OH)_2)$	15
Magnesiohornblende ferroan	$(Ca_2(Mg_4Fe^{3+})\ (Si_7Al)O_{22}(OH)_2)$	4
Magnetite	$(Fe^{2+}Fe^{3+}O_2)$	2
Ilmenite	$(Fe^{2+}Ti^{4+}O_3)$	1

The data presented here demonstrate that the basalt powder has an interesting amount of aluminum and silica. These indicate that the precursors are adequate to create a geopolymer, as these minerals are responsible for the proper geopolymer structure [20,21].

3. Methodology

3.1. Design of Experiments

For research in every field, the development of experiments is paramount to achieve a result. At any given experiment, a set of variables can or cannot be controlled, with different degrees of interactions and influences on the experiment's outcome. In such a complex scenario, the use of Design of Experiments (DoE) has been widely employed. DoE is a statistical approach used to plan an experiment so that the data can be analyzed to a valid and objective conclusion, as it helps understand the correlations between variables and their interactions [28].

In a DoE, the first step is the experiment goal. It can be the optimization of a process or responses or could be the study on the effect of individual factors or variables on the outcome. After deciding the experiment goal(s), it is necessary to define the boundaries of the experiment. The boundaries could be the temperature range of the curing, from 40 °C to 70 °C as an example. It will define the experimental region. This must be done to each variable that can be controlled, determining the levels for each of the factors.

In this paper is was used to plan the experiment and define the most appropriate mix design for the mixture, aiming for a specific outcome. It allows to understand how the input variables interact with each other and how they influence the output variables. An attractive property of the DoE is that it is possible to optimize the experiment, reducing the number of levels of each variable (factor) or even the number of variables. Thus, assessing only the relevant interactions to the desired outcome, the DoE can generally be represented as in Figure 1.

First, there is the controlled input: these inputs gather all the parameters that are measurable and controlled by the researcher. An example is the solution pH: it is a parameter that it is possible to control and measure, but it remains unchanged throughout all the experiments. Moreover, the uncontrolled input is not measured by the researcher, either because they are by definition unmeasurable or their control is too difficult or useless. As an example, it can be stated that the room temperature variation is an uncontrolled input, and maybe within a specific range, it is irrelevant. The input variables contain the actual parameters that the researcher will control and assess during the experiment, such as curing time and temperature and the amount of each material in the mix.

The outputs are also controlled and uncontrolled. The first one refers to the desired and measured actual results of the experiment, such as compressive strength. The former refers to the results that are either not measured or not accurately measured for any reason.

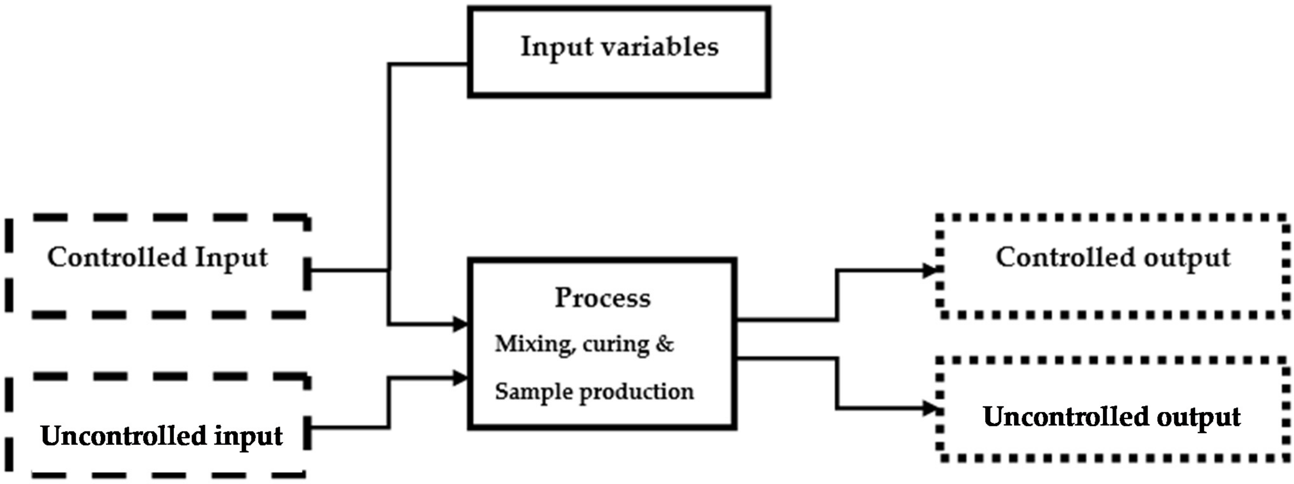

Figure 1. Flow chart of the adopted Design of Experiments (DoE).

It is relevant that when doing any experiment, the researcher is aware of each one of these parameters, especially on the DoE, as these parameters will serve to assess, by statistical analysis, their interaction.

In the present research, the inputs are:

- Controlled input—Mixing time.
- Controlled input—Mixing temperature.
- Uncontrolled input—Air humidity.
- Input variables:
    - Percentage of basalt: it represents the amount of basalt in a MK-and-basalt mix.
    - L/S ratio: it is the ratio between activators (liquid) and precursors (solid).
    - Temperature: it is the controlled temperature used to cure the samples.
    - Time: it is the controlled curing time.

As for the output variables, the controlled and uncontrolled are:

- Controlled output—Fluidity is a measurement of the mortar spread. It gives an indication of how workable the mortar is.
- Controlled output—Success rates the percentage of sound aggregates produced.
- Controlled output—Compressive strength is the resistance unconfined compressive strength of cubic samples.
- Uncontrolled output—Sample humidity.
- Uncontrolled output—Sample leaching.

3.2. Sample Production and Testing Procedure

The procedure adopted for the production and testing of geopolymer samples was conducted as described in the literature [20,21], and it is depicted as a flowchart in Figure 2.

The activators are mechanically mixed for at least 10 min to generate the alkali-activator solution. Then they are mixed for an additional 10 min with the addition of the MK powder; the next step is to mix the obtained paste with the basalt powder for another 3 min at least or until it appears homogeneously mixed. The mortar paste is subsequently tested in terms of workability using a fluidity test; the remaining material is cast into the cubic molds and into artificial aggregates molds. The molds are then placed into the oven at the specified curing temperature and time. After curing, they are removed and unmolded. The artificial aggregates are evaluated in terms of production success rate. At the same time, the cubic samples are placed into plastic tape for an additional seven days' curing at room temperature and then tested for compressive strength.

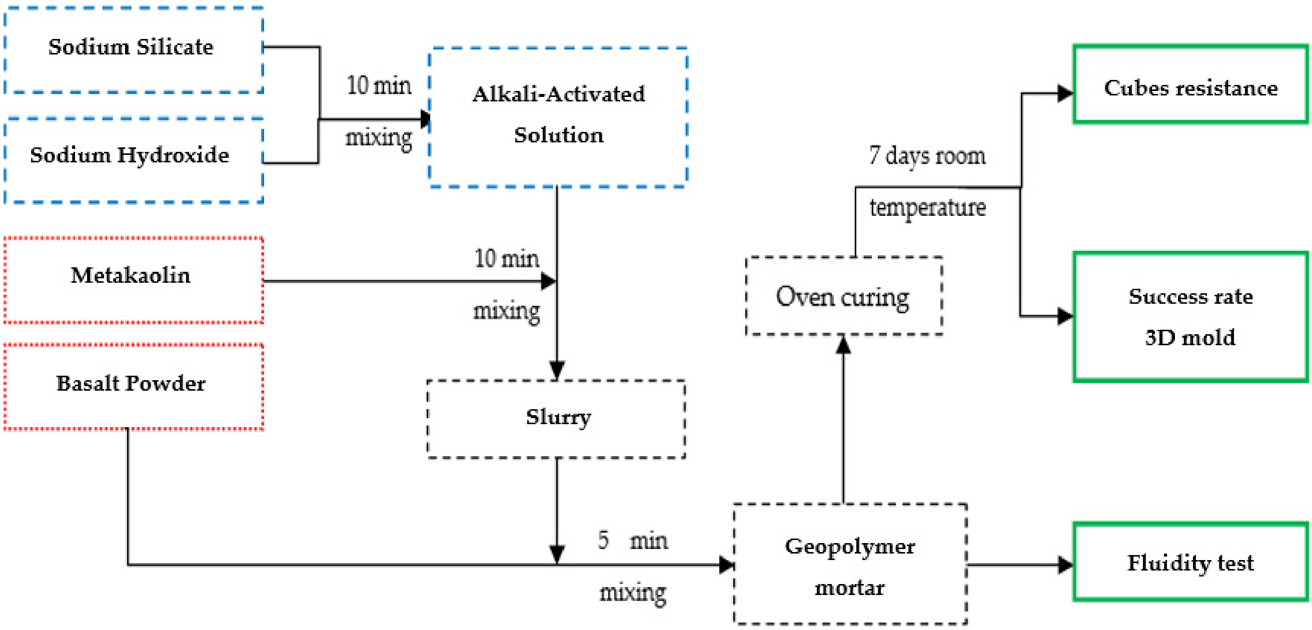

Figure 2. Flowchart of the production and testing procedure.

3.3. Fluidity of Grout According to EN 14824-3: 2012

The fluidity can be considered as an indicator of how easy it would be to inject the mortar mix into the 3D-printed molds in the laboratory. A similar approach shall be used in the case of industrial production. The fluidity test was conducted using as reference the following standard: EN 14824-3: 2012 Grout for prestressing tendons—Part 3: test methods. Even if the reference used is for cement-based grouts, it can give a valid indication of whether the fluidity for geopolymers as a specific standard is still unavailable.

The fluidity (flowability) is measured by the diameter of the circle created by the geopolymer mortar mix flown onto a smooth plate. The test consists of placing the mix into a cylindrical mold with a diameter of 39 mm and 60 mm in height. The cylinder is made of plastic or steel (if used it is necessary to clean it immediately), and the base plate should be smooth.

This cylinder is placed onto the plate surface, filled with the mortar, and moved upward at about 15 cm for a maximum of 30 s. The material spreading should be measured in two different perpendicular directions. The mean diameter is calculated by the average of the two measurements. In Figure 3, it is possible to see the cylinder with the mortar mix inside and ready for testing; other pictures show the spread material being measured in diameter.

3.4. Success Rate of Aggregates Production

As the mortar was used to manufacture artificial aggregates with a specific geometrical design, it was necessary to evaluate the production success rate. In order to quantify it, a simple visual test was conducted after the curing process; the samples were unmolded, and each artificial aggregate was classified as "good" or "bad" on a subjective basis. Suitable aggregates were the ones that kept the desired shape and presented no visible holes or imperfections, while bad ones were those that had any kind of visible defect. Figure 4 serves as an example of the visual test and shows some considered defects from production. Thus, the success rate is the percentage of aggregates with good quality.

Figure 3. Fluidity testing for geopolymer mortars' fluidity.

The present method for classification cannot be applied to mass production for obvious reasons. Therefore, it is suggested to use the sieving technique to select the aggregates with the most appropriate shape and separate them from those with significant failures.

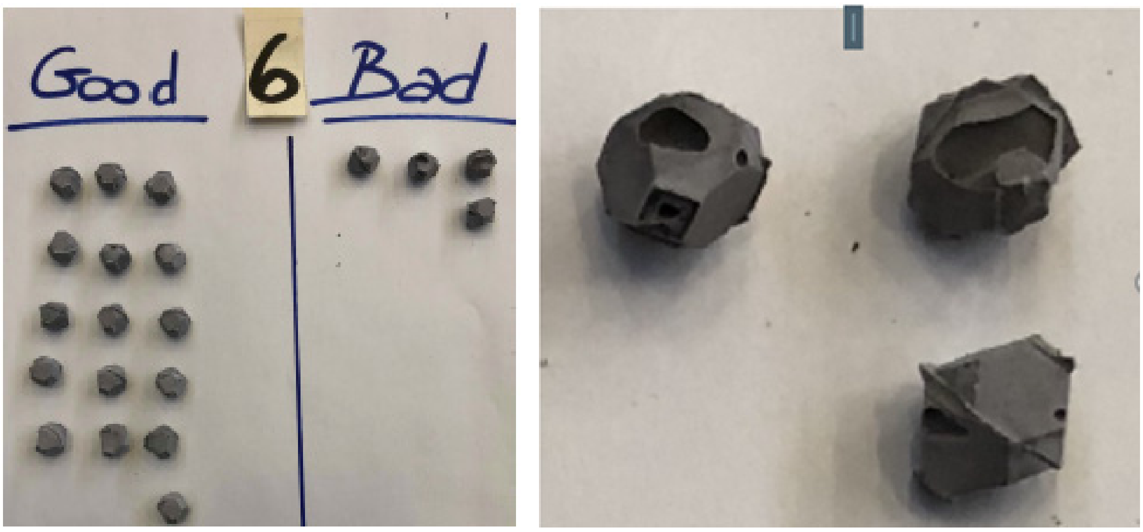

(**a**) (**b**)

Figure 4. Success rate example over production of 20 aggregates: (**a**) classification of aggregates; (**b**) failure examples.

3.5. Compressive Strength: EN 1015-11: 2019

The selected mechanical test was the unconfined compressive strength on geopolymer hardened cubes of 40 mm side length. The cubic samples were cast and cured as instructed in the DoE. The compressive strength was measured as described in the EN 1015-11 standard by means of a hydraulic press (Figure 5) at constant load speed.

As for the surface treatment in the cubic samples, it was unnecessary as the samples are completely smooth without peaks or holes (Figure 5), and a preload of 5 daN was always applied before running the tests. The compressive resistance for each type of mixture of the DoE is calculated as the average strength of four tested cubes.

(**a**) (**b**)

Figure 5. Compressive strength of geopolymer cubes: (**a**) sample in hydraulic press; (**b**) cubic sample before the test.

4. Testing Results and Analysis of the DoE Approach Outcomes

The input variable used in the DoE is shown in Table 2. The first column corresponds to the run order of the experiments, while the second lists the amount of basalt in percent (for instance, 60% basalt means a 40% MK). Other columns are the ratio between the activators and precursors (L/S), the curing temperature in °C, and the curing time in hours.

Table 2. Design of Experiments input variables.

Run Order	Basalt (%)	L/S Ratio	Oven Temperature (°C)	Curing Time (h)
1	80	0.50	50	6
2	90	0.65	50	2
3	80	0.65	60	8
4	90	0.50	60	4
5	90	0.60	70	8
6	70	0.55	50	8
7	80	0.55	70	4
8	70	0.65	40	4
9	80	0.60	40	2
10	60	0.55	60	2
11	70	0.60	60	6
12	60	0.55	40	8
13	60	0.60	50	4
14	90	0.55	40	6
15	60	0.65	70	6
16	70	0.50	70	2

Every single mix was produced and tested for the fluidity of the geopolymer paste, for compressive strength on cubes, and for success rate on aggregates as described in Figure 2; results are listed in Table 3.

For each run order, three samples were used to calculate the average grout spread. As for the compressive strength, four samples were used to calculate the average. As for the success rate, it was assessed by the overall production for each run order.

The percentage variation is presented on the table for the grout spread method and compressive strength.

Table 3. Results obtained for the controlled output variables.

Run Order	Grout Spread Method (cm) [29]	Percentage Variation (%)—Grout Spread Method (cm) [29]	Compressive Strength (Mpa) [30]	Percentage Variation (%)—Compressive Strength (MPa) [30]	Success Rate (%)
1	5.30	13	17.27	9	25
2	13.55	1	0.67	14	85
3	11.75	1	13.11	4	75
4	8.75	4	5.26	3	75
5	12.50	0	1.60	4	20
6	5.35	1	36.59	14	80
7	8.85	1	11.99	9	95
8	10.50	8	35.56	18	55
9	10.70	1	22.70	11	25
10	-	-	39.74	16	0
11	8.80	8	29.37	9	50
12	-	-	45.82	10	0
13	5.55	11	44.33	22	40
14	11.20	0	4.49	10	45
15	8.20	3	35.51	19	100
16	-	-	25.89	23	0

The analysis of results made for each output variable shows:

- Grout spread method (fluidity) [29]:
- Samples 10, 12, and 16 did not provide any measurable results because the mixture was very viscous and did not flow through the mold in the standard specified time.
- Samples 2 and 5 achieved the largest fluidity diameters.
- The higher the fluidity, the easier it is to pour the mortar into the mold.
- Compressive strength [30]:
- Samples 12 and 13 achieved the highest compressive strength.
- Samples 2, 5, and 14 recorded the lowest results.
- Rate of success:
- Samples 10, 12, and 16 gave no results, as the material was not injectable into the aggregates molds.
- Samples 7 and 15 achieved the best results with over 95% suitable aggregates.

It is important to note that results do not allow an easy understanding of how the input variables interact and which would be the most appropriate mix design. However, due to the use of the DoE approach, it is possible to assess the input variables' behavior and their influence on the output variables. The series of graphs called Prediction Profiler from JMP® software (Version 14.0. SAS Institute Inc., Cary, NC, USA, 1989–2019) allow to understand how each input variable influences each of the output variables.

The light red shadow scale represents the confidence interval of each input variable to the corresponding output variable. The red line indicates the relation between the variables, and its tilt means in which way it interacts. Tilted from bottom to top it shows a positive interaction, from top to bottom—negative, the horizontal line indicates that there is no interaction. The cloud of points shows the real data position in relation to the pair of the input and output variables.

From Figure 6 it can be asserted that unconfined compressive strength (UCS) has an opposite relation to the basalt content, meaning that the increase in basalt content would decrease the UCS value. The temperature has an inverse relation to the UCS.

The cured samples were taken out of the oven after the determined time, wrapped in plastic film, and left to cure at room temperature for seven days, and all of them were tested at the same age. The curing time and temperature input variables had little influence on the compressive strength. This might be due to the MK used, which was not very reactive. Therefore, further study is needed on this topic.

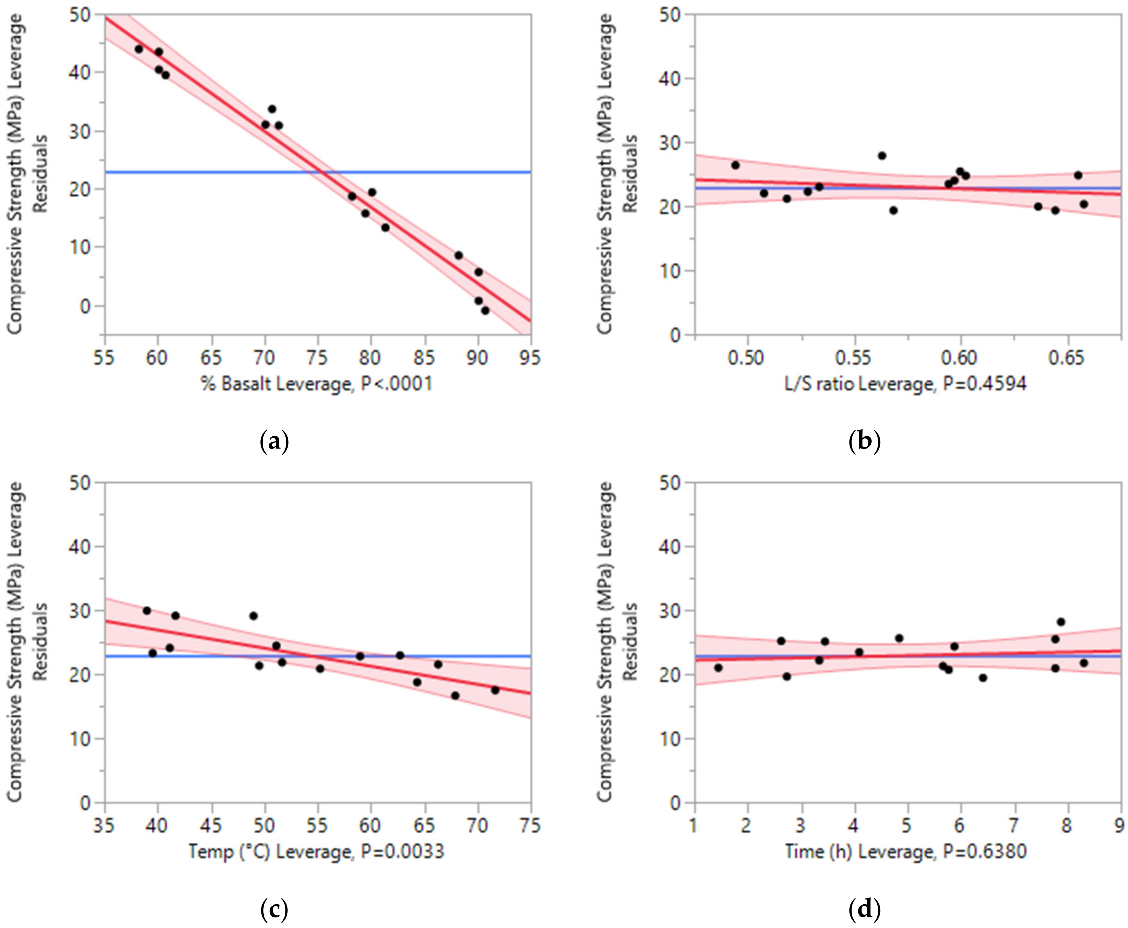

Figure 6. Input variables sensibility and influence on the Unconfined Compressive Strength (UCS): (**a**) basalt leverage; (**b**) L/S ratio leverage; (**c**) temp (°C) leverage; and (**d**) time (h) leverage (Software JMP 14).

With the parameter estimates, it is possible to evaluate their importance in a future model. Table 4 shows each term's parameter estimate, standard error, and probability for the compressive strength. The lower the probability is, the more reliable the input variable is to the model prediction, the most suitable values are identified with an asterisk. The estimate is related to how strong its importance is in the model, and standard error shows how good of a fit there is of the data in relation to the regression line. The lower the number, the better it is.

Table 4. Equation terms estimation and probability for predicting compressive strength.

Term	Estimate	Std Error	Probability > |t|
Intercept	142.14414	10.75799	<0.0001 *
% Basalt	−1.304961	0.068342	<0.0001 *
L/S ratio	−11.35938	14.76356	0.4594
Temperature (°C)	−0.282461	0.073818	0.0033 *
Time (h)	0.1791016	0.369089	0.6380

* Values with acceptable significance.

In Figure 7, it is possible to note that the confidence shadow is too wide, thus meaning that the input variables have a minor relation to the output variables. Nevertheless, it is possible to note that basalt, L/S, and temperature have a minor positive influence.

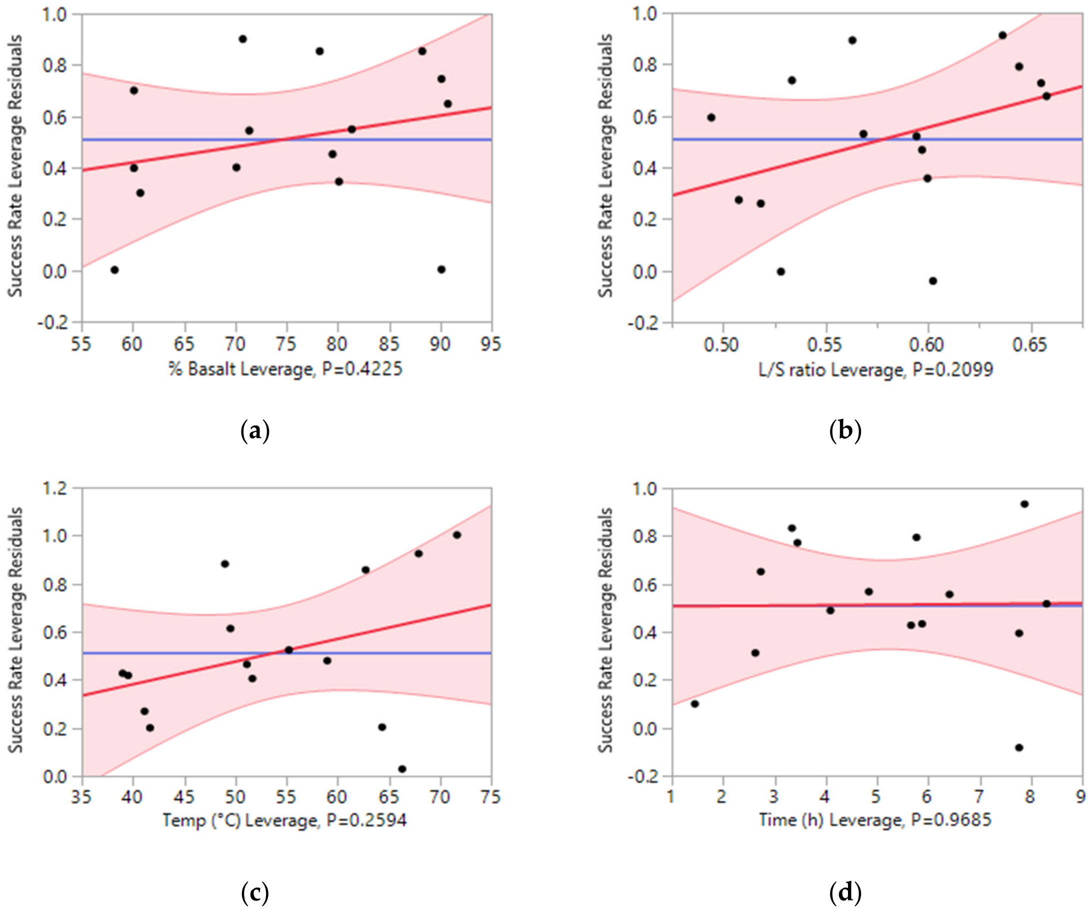

Figure 7. Input variables sensibility and influence on the success rate: (**a**) basalt leverage; (**b**) L/S ratio leverage; (**c**) temp (°C) leverage; and (**d**) time (h) leverage (Software JMP 14).

It is noted in Table 5 that the input variables have no influence on the output variables, as can be seen with the probability values. This might be due to the way the experiment was designed or a lack of sufficient data to assess its interaction.

Table 5. Equation terms estimation and probability for predicting success rate.

Term	Estimate	Std Error	Probability > |t|
Intercept	−1.690266	1.149447	0.1722
% Basalt	0.0061064	0.007302	0.4225
L/S ratio	2.1138298	1.577426	0.2099
Temperature (°C)	0.0094309	0.007887	0.2594
Time (h)	0.0015957	0.039436	0.9685

As for the grout spread method (Figure 8), it is noted that the temperature and time variables are not relevant to the test as it is performed prior to the curing. The other variables have a high interaction probability, thus making it possible to assess their interactions.

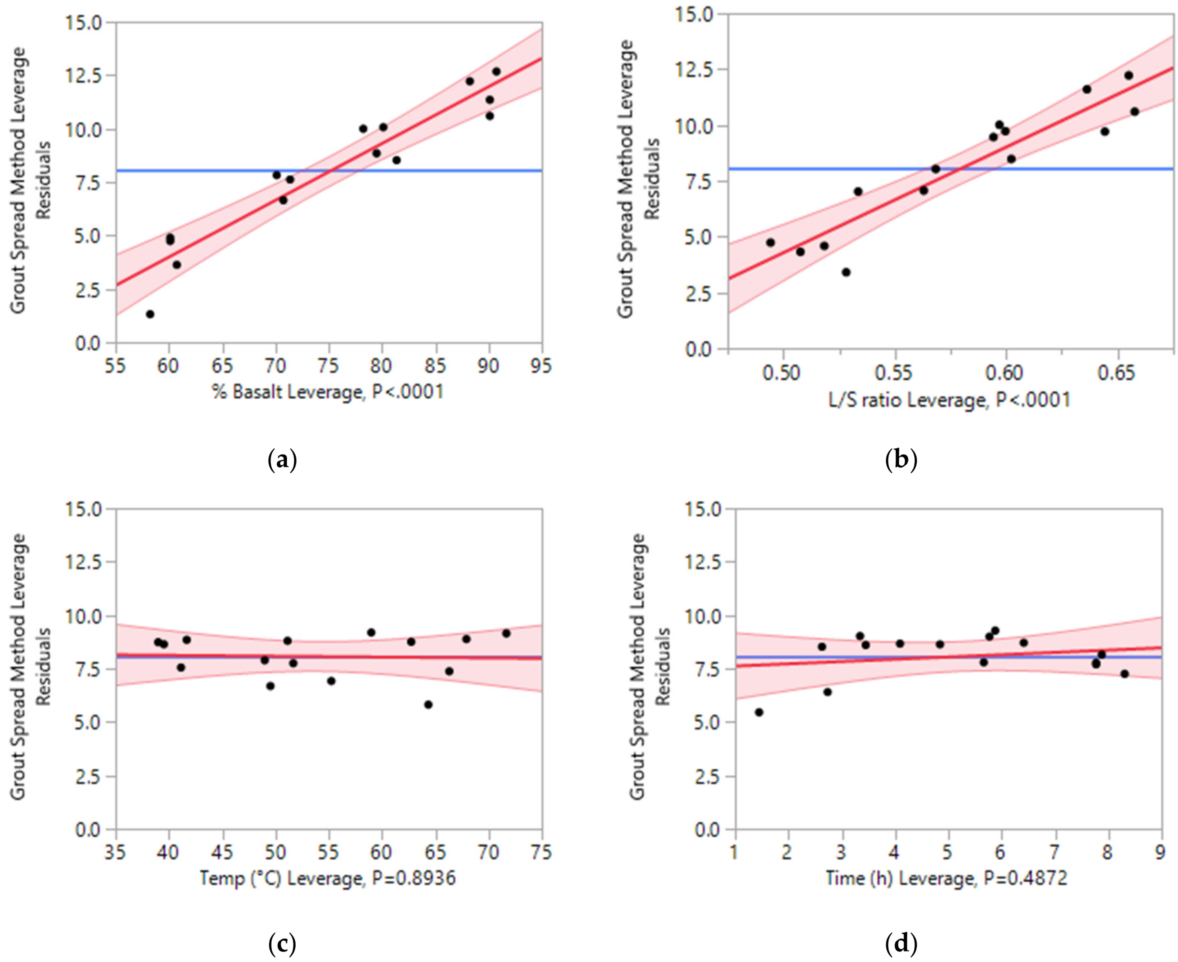

Figure 8. Input variables sensibility and influence on the grout spread method: (**a**) basalt leverage; (**b**) L/S ratio leverage; (**c**) temp (°C) leverage; and (**d**) time (h) leverage (Software JMP 14).

In Table 6, it is possible to note, as stated before, that both temperature and time do not have a reasonable probability, which is entirely correct, as these input variables have not influenced the output variable being assessed. Moreover, intercept, basalt, and L/S ratio have an appropriate probability value, meaning that these variables are intrinsically related to the measured output variable (grout spread method).

Table 6. Equation terms estimation and probability for predicting the grout spread method.

Term	Estimate	Std Error	Probability > |t|
Intercept	−39.71713	4.303934	<0.0001 *
% Basalt	0.2656011	0.027341	<0.0001 *
L/S ratio	47.310638	5.906438	<0.0001 *
Temperature (°C)	0.004053	0.029532	0.8936
Time (h)	0.106516	0.147661	0.4872

* Values with acceptable significance.

The model of compressive strength suffices to select a mix design since the grout spread method and success rate are indicators of the workability of the mortar. Avoiding the points with low grout spread results and aiming for the higher success rate values is possible to narrow the input variables suitable to be used in the model for compressive strength.

With the analysis of the input and output variables interactions in Figure 6 and Table 4, it was possible to develop a model for the compressive resistance, as given in Equation (1).

$$CR(\text{MPa}) = 142.3 - 1.30 \times Basalt - 11.36 \times Liquid - 0.28 \times Temperature(°\text{C}) + 0.18 \times Time(\text{h}) \quad (1)$$

The graph in Figure 9 plots the laboratory-measured compressive strength against the DoE-predicted one. The regression model between the two variables as a valid correlation (R^2 = 0.975), thus providing results within acceptable confidence in the calculated confidence interval.

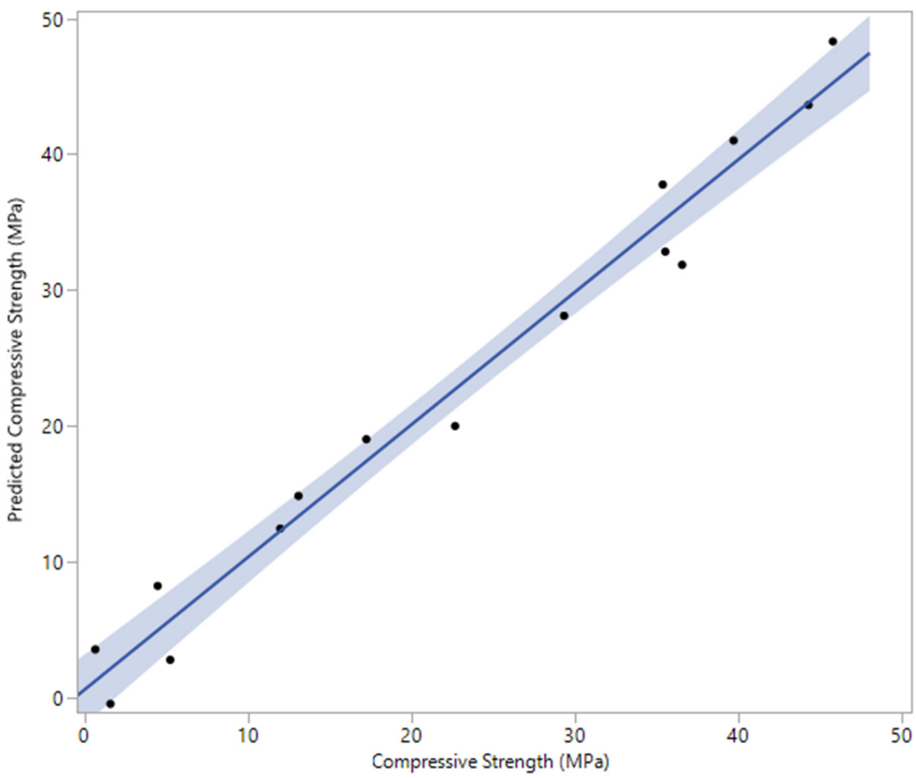

Figure 9. Predicted compressive strength vs. measured compressive strength with fitness shadow.

The shadow represents the confidence interval on how accurate the model is. Some points are out of confidence due to the estimation error of 5%.

The DoE method allows to identify the most relevant input variables: how these are interrelated among them and which is their influence on the output variables. Therefore, it is possible to select a statistically optimized mix design and curing procedure to achieve a minimum desired compressive strength while considering a proper fluidity and success rate for the production of the artificial aggregates in the laboratory. This approach should eventually yield into sound, regularly shaped, and well-cemented aggregates.

As a concluding step for the applied DoE approach, a new set of 14 identical mixes with four cubic samples each were produced and tested to confirm the model accuracy. Each sample was submitted to the compressive strength test, and an average of them was calculated. For these samples, the mix design selected was: 70% basalt (30% MK), 0.5 L/S, 50 °C, and 2 h curing in the oven. According to Equation (1), the compressive strength should be 31.35 MPa with a confidence interval of 95%.

The results of the new samples made with this selected mix are presented in Figure 10. Out of fourteen, only for two samples the recorded compressive strength was lower than the predicted value, but only one lower than the confidence interval of 95%, represented as a dashed red square in Figure 10.

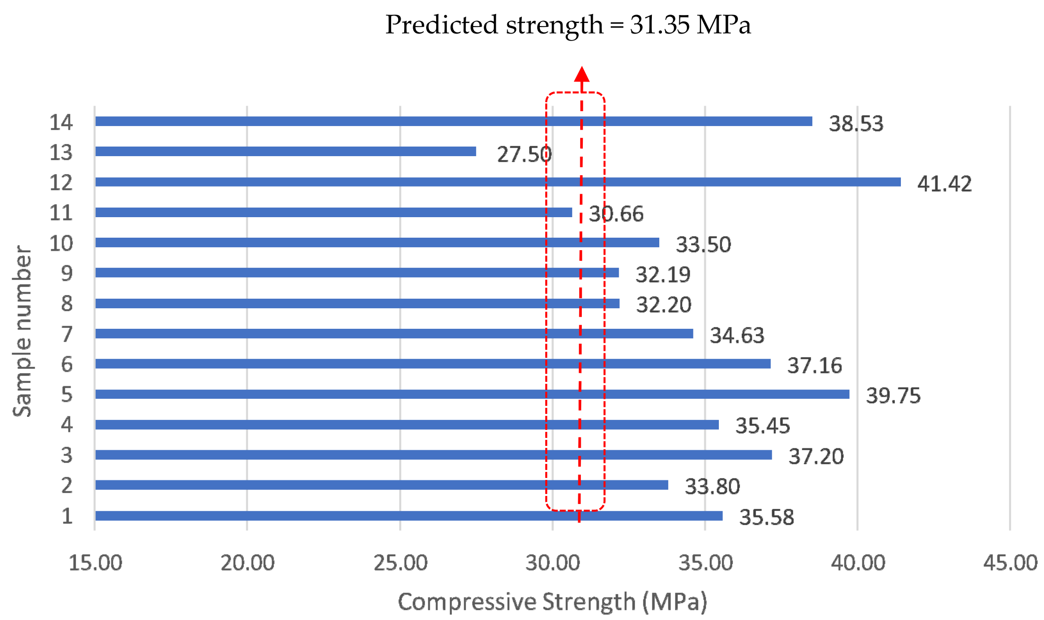

Figure 10. DoE results in confirmation by compressive strength tests on additional samples.

The success rate and grout were measured for the 14 samples, and it is noted that their values are over the expected, as presented in Table 3. It is due mainly to the uncontrolled output variables, such as an increase in room temperature, humidity, and MK quality, and the operator experience.

It is necessary to run more tests with more controlled variables to assess the significance of the input variables for grout spread and success rate.

5. Conclusions

The present paper proposes the preliminary use of the DoE statistical approach to optimize a geopolymer mix design with different proportions of precursors, activators, as well as selected temperatures and time for curing. This is done in order to understand how the input variables reciprocally interact and what their possible output is. The final goal is to choose a mix design and curing process that leads to a workable mixture, which is able to reach an adequate compressive strength while using as much basalt powder as possible, and minimizing the curing time and temperature. The mechanical strength is considered essential for the possible production of sound and durable artificial aggregates. Furthermore, the maximization of basalt content and the minimization of curing time and temperature are essential to reduce the carbon footprint of the final material.

The following conclusions can be drawn from this preliminary study:

- The DoE used was satisfactory because it provided a reliable model to predict the compressive resistance of the proposed materials.
- According to the proposed statistical model, the temperature has little influence on the final resistance. This is debatable as the literature says otherwise. In this research, this might be due to the quality of the MK. Further studies are necessary with a different MK.
- The model helps the researcher to select the most appropriate mix design.
- The model is only relevant for this specific DoE, and it is necessary to change it if the materials used are different.
- The laboratory workability is here directly related to the success rate in the production of aggregates. A material with low workability (fluidity) was found to be difficult to inject into the aggregate's molds. These processes will more likely change at a larger production scale and so will be for the required fluidity. A new DoE will be necessary.
- Overall, the adopted DoE approach provided the authors with consistent information on how each variable behaves and interacts with the final material's characteristics.
- In light of the above, the work on the production of geopolymeric artificial aggregates from waste powders will continue. Aiming for the construction of engineered pavement surfaces that brings benefits in terms of skid resistance (road safety) and noise abatement, the large-scale production of artificial aggregates is envisaged in the near future of this research.

Author Contributions: Conceptualization, S.C.C., P.T., and C.S.; methodology, S.C.C.; software, S.C.C.; validation, P.T.; formal analysis, S.C.C.; investigation, S.C.C., P.T.; data curation, S.C.C.; writing—original draft preparation, S.C.C.; writing—review and editing, P.T., C.S.; supervision, C.S. All authors have read and agreed to the published version of the manuscript.

Funding: This research was funded by the European Union's Horizon 2020 research and innovation program under the Marie Sklodowska-Curie grant agreement N°765057.

Institutional Review Board Statement: Not applicable.

Informed Consent Statement: Not applicable.

Data Availability Statement: All datas have been provided within the article.

Conflicts of Interest: The authors declare no conflict of interest.

References

1. Zaumanis, M.; Arraigada, M.; Wyss, S.A.; Zeyer, K.; Cavalli, M.C.; Poulikakos, L.D. Performance-based design of 100% recycled hot-mix asphalt and validation using traffic load simulator. *J. Clean. Prod.* **2019**, *237*, 117679, doi:10.1016/j.jclepro.2019.117679.
2. Lizárraga, J.M.; Ramírez, A.; Díaz, P.; Marcobal, J.R.; Gallego, J. Short-term performance appraisal of half-warm mix asphalt mixtures containing high (70%) and total RAP contents (100%): From laboratory mix design to its full-scale implementation. *Constr. Build. Mater.* **2018**, *170*, 433–445, doi:10.1016/j.conbuildmat.2018.03.051.
3. Afonso, M.L.; Dinis-Almeida, M.; Fael, C.S. Characterization of the Skid Resistance and Mean Texture Depth in a Permeable Asphalt Pavement. *IOP Conf. Ser. Mater. Sci. Eng.* **2019**, *471*, doi:10.1088/1757-899X/471/2/022029.
4. Sangiorgi, C.; Tataranni, P.; Simone, A.; Vignali, V.; Lantieri, C.; Dondi, G. A laboratory and filed evaluation of Cold Recycled Mixture for base layer entirely made with Reclaimed Asphalt Pavement. *Constr. Build. Mater.* **2017**, *138*, 232–239, doi:10.1016/j.conbuildmat.2017.02.004.
5. Solouki, A.; Viscomi, G.; Lamperti, R.; Tataranni, P. Quarry waste as precursors in geopolymers for civil engineering applications: A decade in review. *Materials* **2020**, *13*, 3146, doi:10.3390/ma13143146.
6. Sangiorgi, C.; Tataranni, P.; Lantieri, C.; Mazzotta, F. Application of Mining Waste Powder as filler in Hot Mix Asphalt. *MATEC Web Conf.* **2019**, *274*, 04002, doi:10.1051/matecconf/201927404002.

7. Barbuta, M.; Bucur, R.D.; Cimpeanu, S.M.; Paraschiv, G.; Bucur, D. Wastes in Building Materials Industry. *Agroecology* **2015**, 2014–2020, doi:10.5772/59933.
8. Sui, Y.; Ou, C.; Liu, S.; Zhang, J.; Tian, Q. Study on properties of waste concrete powder by thermal treatment and application in mortar. *Appl. Sci.* **2020**, *10*, 998, doi:10.3390/app10030998.
9. de Carvalho, J.M.F.; de Melo, T.V.; Fontes, W.C.; dos Santos Batista, J.O.; Brigolini, G.J.; Peixoto, R.A.F. More eco-efficient concrete: An approach on optimization in the production and use of waste-based supplementary cementing materials. *Constr. Build. Mater.* **2019**, *206*, 397–409, doi:10.1016/j.conbuildmat.2019.02.054.
10. Paiva, H.; Yliniemi, J.; Illikainen, M.; Rocha, F.; Ferreira, V.M. Mine tailings geopolymers as a waste management solution for a more sustainable habitat. *Sustainability* **2019**, *11*, 995, doi:10.3390/su11040995.
11. Mohajerani, A.; Suter, D.; Jeffrey-Bailey, T.; Song, T.; Arulrajah, A.; Horpibulsuk, S.; Law, D. Recycling waste materials in geopolymer concrete. *Clean Technol. Environ. Policy* **2019**, *21*, 493–515, doi:10.1007/s10098-018-01660-2.
12. Mabroum, S.; Moukannaa, S.; El Machi, A.; Taha, Y.; Benzaazoua, M.; Hakkou, R. Mine wastes-based geopolymers: A critical review. *Clean. Eng. Technol.* **2020**, *1*, 100014, doi:10.1016/j.clet.2020.100014.
13. Losa, M.; Leandri, P.; Bacci, R. Mechanical and Performance-Related Properties of Asphalt Mixes Containing Expanded Clay Aggregate. *Transp. Res. Rec.* **2008**, *2051*, 23–30, doi:10.3141/2051-04.
14. Borges, J.K.; Pacheco, F.; Tutikian, B.; de Oliveira, M.F. An experimental study on the use of waste aggregate for acoustic attenuation: EVA and rice husk composites for impact noise reduction. *Constr. Build. Mater.* **2018**, *161*, 501–508, doi:10.1016/j.conbuildmat.2017.11.078.
15. Callai, S.C.; Sangiorgi, C. A review on acoustic and skid resistance solutions for road pavements. *Infrastructures* **2021**, under review.
16. Manaf, M.B.H.A.; Abdul Razak, R.; Muhamad, K.; Abdul Rahim, M.; Ahmad, M.M.; Hao, T.P. A study on the potential of geopolymer artificial aggregate as substitute for granite and limestone aggregate. *IOP Conf. Ser. Earth Environ. Sci.* **2020**, *476*, doi:10.1088/1755-1315/476/1/012034.
17. George, G.K.; Revathi, P. Production and Utilisation of Artificial Coarse Aggregate in Concrete—A Review. *IOP Conf. Ser. Mater. Sci. Eng.* **2020**, *936*, doi:10.1088/1757-899X/936/1/012035.
18. Tataranni, P.; Sangiorgi, C. Synthetic aggregates for the production of innovative low impact porous layers for urban pavements. *Infrastructures* **2019**, *4*, 48, doi:10.3390/infrastructures4030048.
19. Cerveira, A.; Correia, E.; Cristelo, N.; Miranda, T.; Castro, F.; Fernández-Jiménez, A. Statistical Analysis of the Influence of Several Factors on Compressive Strength of Alkali Activated Fly Ash. *Procedia Struct. Integr.* **2017**, *5*, 1116–1122, doi:10.1016/j.prostr.2017.07.099.
20. Provis, J.L.; Rees, C. *Geopolymers: Structures, Processing, Properties and Industrial Applications*; Woodhead Publishing: Cambridge, UK, 2009.
21. Davidovits, J. *Geopolymer Chemistry and Application*, 4th ed.; Institut Geopolymere: Saint-Quentin, France, 2015.
22. Liu, Z.; Cai, C.S.; Liu, F.; Fan, F. Feasibility Study of Loess Stabilization with Fly Ash–Based Geopolymer. *J. Mater. Civ. Eng.* **2016**, *28*, 04016003, doi:10.1061/(asce)mt.1943-5533.0001490.
23. Jiao, X.; Zhang, Y.; Chen, T.; Bao, S.; Liu, T.; Huang, J. Geopolymerisation of a silica-rich tailing. *Miner. Eng.* **2011**, *24*, 1710–1712, doi:10.1016/j.mineng.2011.09.008.
24. Siddique, R.; Klaus, J. Influence of metakaolin on the properties of mortar and concrete: A review. *Appl. Clay Sci.* **2009**, *43*, 392–400, doi:10.1016/j.clay.2008.11.007.
25. Aboulayt, A.; Riahi, M.; Ouazzani Touhami, M.; Hannache, H.; Gomina, M.; Moussa, R. Properties of metakaolin based geopolymer incorporating calcium carbonate. *Adv. Powder Technol.* **2017**, *28*, 2393–2401, doi:10.1016/j.apt.2017.06.022.
26. Medri, V.; Papa, E.; Lizion, J.; Landi, E. Metakaolin-based geopolymer beads: Production methods and characterization. *J. Clean. Prod.* **2020**, *244*, 118844, doi:10.1016/j.jclepro.2019.118844.
27. Longhi, M.A.; Rodríguez, E.D.; Walkley, B.; Zhang, Z.; Kirchheim, A.P. Metakaolin-based geopolymers: Relation between formulation, physicochemical properties and efflorescence formation. *Compos. Part B Eng.* **2020**, *182*, doi:10.1016/j.compositesb.2019.107671.
28. Romagnoli, M.; Leonelli, C.; Kamse, E.; Lassinantti Gualtieri, M. Rheology of geopolymer by DOE approach. *Constr. Build. Mater.* **2012**, *36*, 251–258, doi:10.1016/j.conbuildmat.2012.04.122.
29. *BSI Standards Publication Grout for Prestressing Tendons Part 3: Test Methods*; British Sandards Institution: London, UK, 2012.
30. *EN 1015-11 BSI Standards Publication Methods of Test for Mortar for Masonry*; British Sandards Institution: London, UK, 2019.